Vehicle System Dynamics
2003, Vol. 00, No. 0, pp. 000–000

0042-3114/03/0000-000$16.00
© Swets & Zeitlinger

A Fuzzy Logic Direct Yaw-moment Control System for All-Wheel-Drive Electric Vehicles

FARZAD TAHAMI[1], SHAHROKH FARHANGI[2] AND REZA KAZEMI[3]

SUMMARY

In-wheel-motors are revolutionary new electric drive systems that can be housed in vehicle wheel assemblies. Such E-wheels permit packaging flexibility by eliminating the central drive motor and the associated transmission and driveline components, including the transmission, the differential, the universal joints and the drive shaft. Apart from many advantages of such a system, unequalled independent wheel control allows vehicle dynamic improvement to assist the driver in enhancing cornering and straight-line stability on slippery roads and in adverse ground conditions. In this paper a Fuzzy logic driver-assist stability system for all-wheel-drive electric vehicles based on a yaw reference DYC is introduced. The system assists the driver with path correction, thus enhancing cornering and straight-line stability and providing enhanced safety. A feed-forward neural network is employed to generate the required yaw rate reference. The neural net maps the vehicle speed and the steering angle to give the yaw rate reference. The vehicle true speed is estimated using a multi-sensor data fusion method. Data from wheel sensors and an embedded accelerometer are fed into an estimator, where a Fuzzy logic system decides which input is more reliable. The efficiency of the proposed system is approved by conducting a computer simulation. The proposed control system is an effective and easy to implement method to enhance the stability of all-wheel-drive electric vehicles.

1. INTRODUCTION

An innovative configuration for electric vehicles is all-wheel-drive EV, in which each wheel is driven individually by electric wheels (E-wheels). Even electric motors can be housed in vehicle wheel assemblies usually known as In-Wheel motors. E-Wheel systems have been recognized as a break-through concept that will have a major impact on future electric and hybrid vehicle design. The design eliminates traditional

[1]Address correspondence to: Farzad Tahami, Jovain Electrical Machines Co., 3rd alley Khaled Islamboly St., Tehran 15136, Iran. Tel.: +98-21-8727054; Fax: +98-21-8724498; E-mail: farzad_tahami@yahoo.com
[2]University of Tehran, North Kareghar Ave., Tehran, Iran. Tel.: +98-21-2546391; Fax: +98-21-8778690; E-mail: farhanghi@ece.ut.ac.ir
[3]KN Toosi University of Technology, East Vafadar St., Tehran, Iran. Tel.: +98-21-7344010; Fax: +98-21-7334338; E-mail: r.kazemi@ikco.com

VSM10-02

drive-train components, including the transmission, the differential, universal joints and driveshaft as well as a central motor. By placing the motors in the wheels, there is more space for batteries, auxiliary power unit or fuel cells, along with more cargo and passenger space. It also provides space to meet an ever increasing demand for onboard electrical systems and fuel cell equipment. The electric drive system can be used in battery powered electric vehicles, both autonomous and grid connected hybrid electric vehicles and fuel cell vehicles. The system also reduces overall vehicle weight, lowers costs, and provides highly efficient and effective regenerative braking. It is ideally suited for drive-by-wire vehicle of the future and provides important new safety features through significantly increased vehicle control. Indeed, the distributed control system and the direct drive features provide independent wheel control in both acceleration and braking, results in easy integration of ABS, traction and stability control systems. Torque of each wheel can be adjusted according to road grip and the amount of power or braking needed to maintain constant traction. Independent driven wheels provides another steering control input, i.e. the torque steering. The vehicle yaw rate can be controlled by this steering method, which is usually referred as Direct Yaw-moment Control (DYC). It has been proved that DYC is more effective in enhancing vehicle stability than four wheel steering [1]. Actually, the yaw moment resulting from difference in longitudinal tire force of left and right wheels is insignificantly influenced by lateral acceleration [2]. However, most studies do not guarantee the robustness to uncertainty in vehicle parameters and disturbances that are intrinsically associated with the vehicle and the road [3–5].

In this paper, a Fuzzy logic controller is used in order to control the yaw rate. Another Fuzzy controller is employed to prevent the tire forces being saturated due to the additional torque applied by the yaw controller. The use of Fuzzy logic is rapidly spreading in order to satisfy the following requirements: (1) to develop control systems with nonlinear characteristics and decision making systems for controllers, (2) to cope with an increasing number of sensors and exploit the larger quantity of information, (3) to reduce development time, (4) to reduce costs associated with incorporating the technology into the product. Vehicle dynamics and braking systems are complex and behave strongly non-linear which causes difficulties in developing a classical controller system. Fuzzy logic however facilitates such system designs and improves tuning abilities. The authors have already developed a new approach to improve the stability of 2WD and 4WD electric vehicles using Fuzzy logic [6, 7].

The yaw controller impels the vehicle to pursue a reference yaw rate. In previous works the authors employed a simplified vehicle model to generate a reference yaw rate [6, 7]. In this paper the yaw reference is generated by a well trained neural network. Neural reinforcement learning algorithms have been shown to be very useful in situations in which it is not possible to give the system explicit instructions as to exactly how it should go about improving its performance. A crucial realization is that

the substitute, or emulator, need not compute the map exactly, but merely approximate it to a degree of precision that preserves the perceived faithfulness of the resulting reference to the simulated yaw dynamics of the vehicle. The authors' premise is that, to a sufficient degree of accuracy and at significant computational savings, trained neural networks can approximate maps not just for simple dynamical systems, but also for those associated with complex vehicle dynamic models.

2. CONTROL SYSTEM DESIGN

2.1. Yaw Rate Controller

In an oversteer condition, the vehicle rotates more than the driver command and this could result in the rear of the vehicle becoming ''loose'' or sliding outward. Understeer conditions, or ''pushing,'' results when the front tires of the vehicle are not cornering as fast as the rear of the vehicle. Apart from these sources of instability, an uneven longitudinal tire force may have a significant undesired effect on vehicle yaw motion.

In above conditions the yaw control system intervenes either by increasing or decreasing the torque at each individual wheel. This creates a counter yaw moment that will rotate the vehicle in the opposite direction of the spin and maintaining the driver's control.

Considering the forces acting on the vehicle, as depicted in Fig. 1, one can write the vehicle yaw motion equation as follows:

$$\begin{aligned} I_z\dot{r} = {} & (I_x - I_y)pq + L_f[F_{x1}\sin(\delta_{f1}) + F_{y1}\cos(\delta_1) + F_{x2}\sin(\delta_2) + F_{y2}\cos(\delta_2)] \\ & - L_r(F_{y3} + F_{y4}) + \frac{T_f}{2}[F_{x1}\cos(\delta_1) - F_{y1}\sin(\delta_1) - F_{x2}\cos(\delta_2) \\ & + F_{y2}\sin(\delta_2)] + \frac{T_r}{2}(F_{x3} - F_{x4}) + \sum_{i=1}^{4} M_{zi} \end{aligned} \tag{1}$$

Where r, p and q denote the angular velocities corresponding to yaw, roll and pitch angles. I_x, I_y, and I_z are the vehicle moment of inertia about the x, y, and z axes and M_z is the tire self-aligning torque.

Rearranging Equation [1] and assuming small and equal steering angles for the front wheels and no steering for the rear wheels, one can write:

$$I_z\dot{r} = (I_x - I_y)pq + L_f F_{yf} - L_r F_{yr} + \frac{T_f}{2}\Delta F_{xf} + \frac{T_r}{2}\Delta F_{xr} + \sum_{i=1}^{4} M_{zi}$$

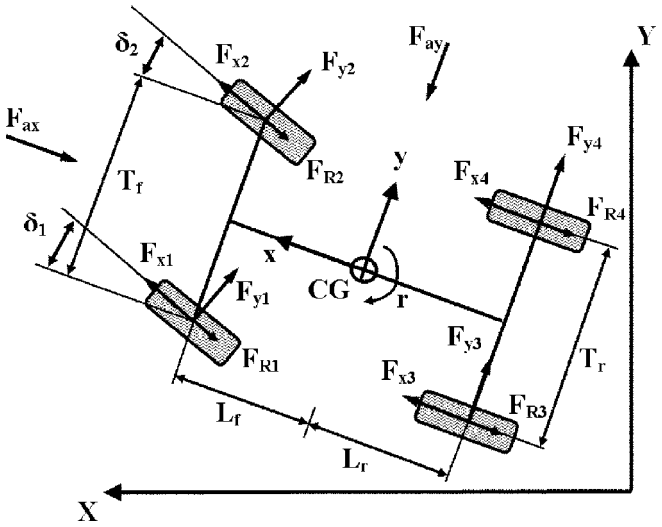

Fig. 1. Forces acting in the horizontal plane.

Where ΔF_{xf} and ΔF_{xr} are the differences in the longitudinal force of left and right wheels in the front and the rear:

$$\Delta F_{xf} = F_{x1} - F_{x2}$$
$$\Delta F_{xr} = F_{x3} - F_{x4}$$

And F_{yf} and F_{yr} are the total lateral forces in the front and rear wheels.

$$F_{yf} = F_{y1} + F_{y2}$$
$$F_{yr} = F_{y3} + F_{y4}$$

Hence, applying a differential input torque to the right and left side wheels can directly control the yaw rate.

A Fuzzy logic controller is used to keep the yaw rate in a desired value; r_d. Fuzzy control is used because it can provide robust response even with significant uncertainties in tire-road model. The controller has two input signals, the loop error $e = r - rd$ and the error rate of change. The control output is the deviation in the applied torque to the motors. Fig. 2 shows the block diagram of the vehicle stability assist system. The membership functions in per unit form are depicted in Fig. 3 Table 1 shows the rule base for the Fuzzy yaw rate controller. The input variables are normalized and fuzzified, and then the corresponding control rules are evaluated from membership functions and the rule table. Finally the control rules are defuzzified to derive the control signal.

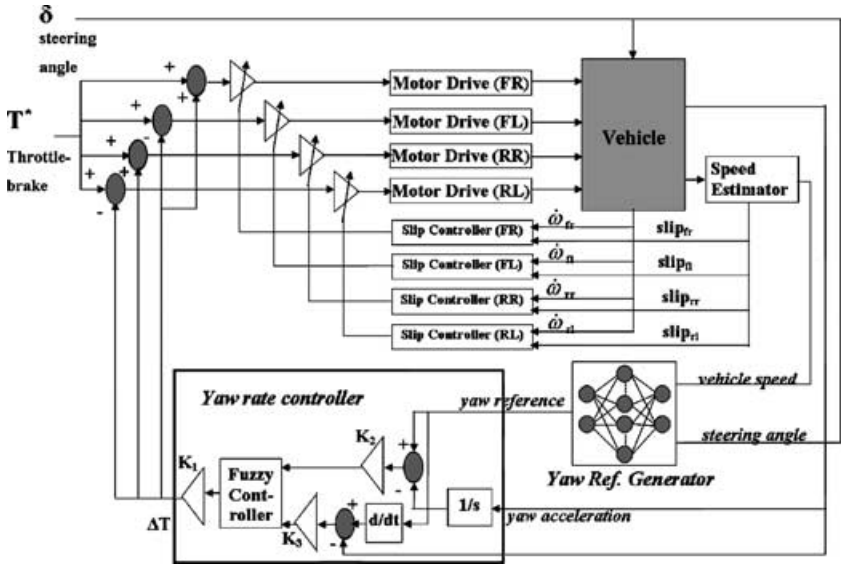

Fig. 2. The proposed yaw motion control system.

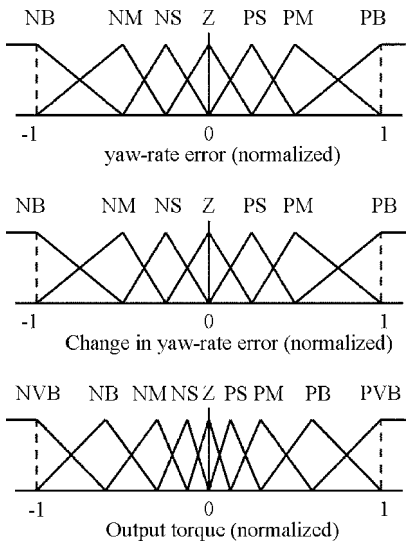

Fig. 3. Membership functions for the yaw rate controller.

Table 1. Fuzzy rule-base for the yaw rate controller.

Change in yaw-rate error	Yaw-rate error						
	NB	NM	NS	Z	PS	PM	PB
NB	NVB	NVB	NVB	NB	NM	NS	Z
NM	NVB	NVB	NB	NM	NS	Z	PS
NS	NVB	NB	NM	NS	Z	PS	PM
Z	NB	NM	NS	Z	PS	PM	PB
PS	NM	NS	Z	PS	PM	PB	PVB
PM	NS	Z	PS	PM	PB	PVB	PVB
PB	Z	PS	PM	PB	PVB	PVB	PVB

2.2. Yaw Reference Generator

From the steady state cornering theory of a single track model, it is known that the yaw velocity of a vehicle satisfies the following equation [8]:

$$r_d = \frac{V}{L + KV^2}\delta$$

Where K is the under-steer gradient, L is the vehicle wheel-base, V is the vehicle speed and δ is the wheel turn angle. A desired yaw rate is assumed to be attainable with neutral steer ($K = 0$), while a correction term is included to modify the result:

$$r_d = \frac{V}{L}\delta + r_{\text{correction}}(\delta, V)$$

The correction term is produced by a feed-forward neural network, which is trained to approximate the desired yaw rate. Certain types of neural networks are universal approximators. A properly trained neural network with adequate neurons can simulate any continues function on a compact domain to any given degree of accuracy.

Figure 4 shows the neural network used for yaw rate reference generation. The net consists of two hidden layers each having 30 neurons. The internal layers have Tan-sigmoid neurons, while the transfer function of the output layer is linear. The neural net maps the vehicle speed and the steering angle to the yaw rate reference. The training process is performed using the results of sine waveform maneuvers with different velocities, which are simulated with a high adhesive road condition. By this maneuver lateral and longitudinal dynamics are exited. The neural net learns to generate the vehicle yawing response based on vehicle speed and steering angle. Since the training is performed with adhesive roads conditions, the neural net demands the same performance from the vehicle on any road condition.

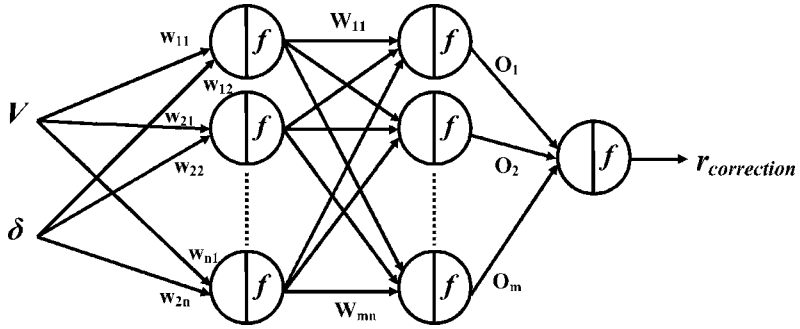

Fig. 4. Neural-network yaw-reference generator.

2.3. Slip Controller

The additional torque applied by the yaw controller may saturate the tire force; hence a slip ratio controller is included in the yaw control loop.

A Fuzzy controller for each wheel is used to keep the slip ratio within its stable region. The inputs to the controller are the wheel slip and the wheel angular acceleration. The Fuzzy rules regard the latter input as a virtual criterion for the direction of slip variations. The output of the controller is the amount of torque weakening that should be devoted to the torque command of the motors, in order to prevent the tire to enter into its saturation region.

Figure 5 shows the membership functions. The rule base of the Fuzzy slip controller is tabulated in Table 2.

2.4. Speed Estimator

A crucial point in the development of wheel slip control systems is the determination of the vehicle speed. To obtain very accurate results, optical or microwave sensors can be used. However, these sensors are very expensive and can not be used for this application. In this paper the vehicle speed is estimated. A data fusion method is used for this purpose. The wheel rotational speeds are used as primary measuring inputs. An additional accelerometer is embedded in the vehicle in order to measure the vehicle longitudinal acceleration. The integral of the acceleration is regarded as another input. The inputs are all fed into an estimator, where a Fuzzy logic determines which input is more reliable. Inputs are weighted and averaged to give the estimated speed. Figure 6 shows the block diagram of the estimator. The estimator consists of two stages. In the first stage, which is referred as preprocessing, the wheel slips are calculated using the previous estimated vehicle speed, wheel angular velocities and

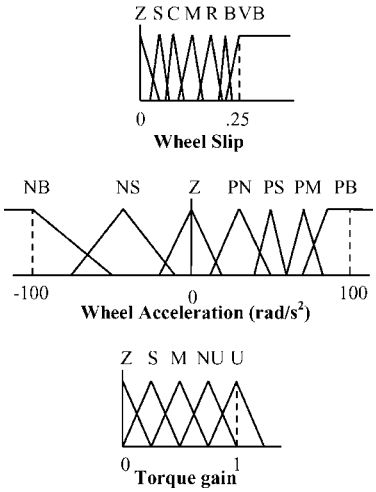

Fig. 5. Membership functions for the slip controller.

Table 2. Fuzzy rule-base for the slip controller.

Wheel acceleration times the sign of slip	Wheel slip (unsigned)						
	Z	S	C	M	R	B	VB
NB	U	U	U	U	U	U	NU
NS	U	U	U	U	U	NU	M
Z	U	U	U	U	NU	M	Z
PN	U	U	U	NU	M	Z	Z
PS	U	U	NU	M	S	Z	Z
PM	U	U	M	S	S	Z	Z
PB	U	NU	S	Z	Z	Z	Z

yaw rate. Assuming small vehicle body side slip angle, the wheel angular velocities are transferred to the vehicle center of gravity for this purpose:

$$V_{RFR} = V_{UFR} - \dot{\psi}\frac{T_f}{2}$$

$$V_{RFL} = V_{UFL} + \dot{\psi}\frac{T_f}{2}$$

$$V_{RRR} = V_{URR} - \dot{\psi}\frac{T_r}{2}$$

$$V_{RRL} = V_{URL} + \dot{\psi}\frac{T_r}{2}$$

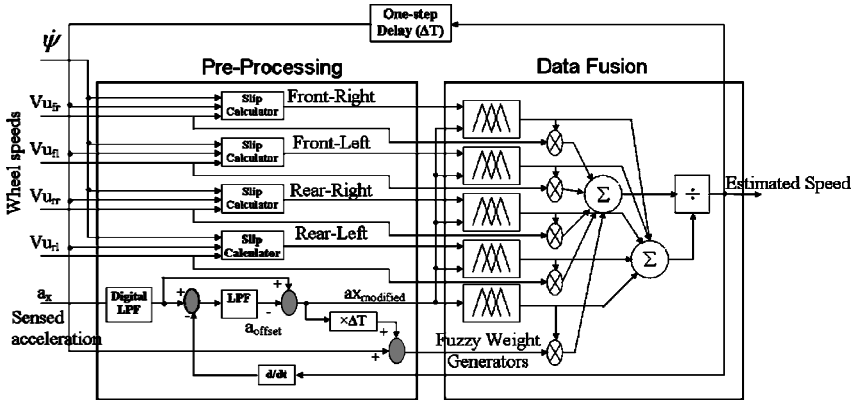

Fig. 6. Block diagram of the speed estimator.

In order to filter out the vibration noise included in the accelerometer's measurement, the measured signal is first fed into a low pass infinite impulse response (IIR) digital filter.

To avoid drifting of integrator, the offset of the accelerometer is rejected by subtracting the derivation of the estimated speed from the measured acceleration and followed by low-pass filtering.

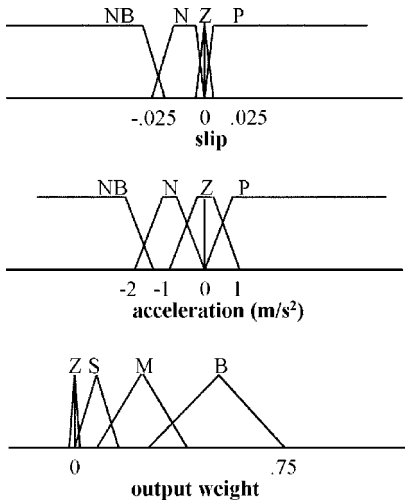

Fig. 7. Membership functions for fuzzification of inputs and the output of speed estimator.

Table 3. Weighting rule sets for: (a) wheels speed, (b) Integration.

Acceleration	(a) Slip			
	NB	N	Z	P
NB	Z	Z	S	Z
N	Z	S	M	Z
Z	Z	S	B	S
P	Z	S	M	S

	(b) Acceleration		
NB	N	Z	P
B	M	S	B

In the next stage, the wheel speeds and the integral of vehicle longitudinal acceleration are weighted using Fuzzy rules. The weighted values are averaged to give the vehicle speed. Figure 7 depicts the membership functions used in Fuzzy weight generators. In Table 3 the rule sets are tabulated. These rules have been established on basis of linguistic terms such as:

- In cruise driving, the integral of the vehicle acceleration is not reliable and minimally weighted, since the accelerometer signal is comparable to offset and noise of the measuring circuit. The wheels are weighted according to their slip.
- In braking situation if a wheel has a small negative slip, then it is slightly weighted, otherwise it is minimally weighted.
- In acceleration, when a wheel has a positive or zero slip it will be slightly weighted, otherwise it will be minimally weighted.

3. MODELING AND SIMULATION

3.1. Vehicle Model

A fourteen-degree of freedom model is used for the simulation purposes, where 6 degrees are devoted to the chassis motion and eight degrees are assigned to the wheels rotational and vertical movement. Figure 8 shows different coordinates that are used for the modeling purpose. All movement of the vehicle body are given with the centre of gravity coordinate system, while there is a coordinate system for each individual wheel. The parameters of the vehicle model are tabulated in Table 4.

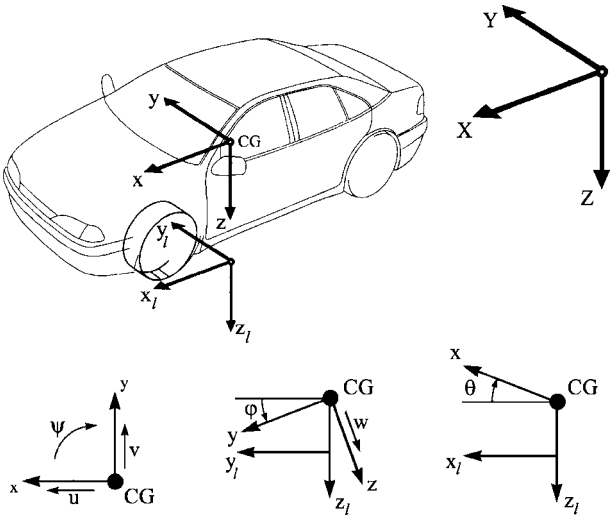

Fig. 8. Coordinate systems for vehicle modeling.

Table 4. Vehicle parameters.

Parameter	Symbol	Unit	Value
Vehicle total mass	M_t	kg	1482.7
Front Unsprung mass	M_{uf}	kg	95.5
Rear Unsprung mass	M_{ur}	kg	108.8
Moments of inertia of total car about X axis	I_x	kg m^2	346.73
Moments of inertia of total car about Y axis	I_y	kg m^2	1675.8
Moments of inertia of total car about Z axis	I_z	kg m^2	1808.8
Moment of inertia of wheels	I_w	kg m^2	2.11
Track width	T	m	1.4375
Distance from front axle to CG	L_f	m	1.2247
Distance from rear axle to CG	L_r	m	1.4373
Height of CG	h_{cg}	m	0.5253
Effective radius of wheels	R_w	m	0.285
Spring constant of front springs	K_{sf}	N/m	15400
Spring constant of rear springs	K_{sr}	N/m	19000
Spring constant of tires	K_u	N/m	175000
Damping coefficient of front dampers	C_{sf}	N s/m	1150
Damping coefficient of rear dampers	C_{sr}	N s/m	6000
Damping coefficient of tires	C_{uf}	N s/m	50
Aerodynamic drag coefficient	C_d	N s/m	0.32

3.2. Tire Model

The accuracy of the simulation results is predominantly determined by the accuracy of the tire model. The desired simulation for the application herein concerned can be carried out by a steady state tire characteristics. The most famous special-function based tire model is the Magic Formula proposed by Bakker, Nyborg and Pacejka [9]. The longitudinal and lateral forces are carried out from the following formula:

$$F_x = D_x \sin\left(C_x \arctan(B_x \Phi_x)\right) + S_{vx}$$
$$F_y = D_y \sin\left(C_y \arctan(B_y \Phi_y)\right) + S_{vy}$$

Where,

$$\Phi_x = (1 - E_x)(\lambda + S_{hx}) + \frac{E_x}{B_x} \arctan(B_x(\lambda + S_{hx}))$$
$$\Phi_y = (1 - E_y)(\alpha + S_{hy}) + \frac{E_y}{B_y} \arctan(B_y(\alpha + S_{hy}))$$

In which λ is the wheel slip and α is slip angle. The other parameters depend on the normal load and factors which are determined from experience. The special function form also applies to the self-aligning torque.

3.3. Suspension Model

A quarter-vehicle model is used for each wheel. A model of the suspension system is shown in Figure 9. Each wheel has an individual mass, which is connected to the

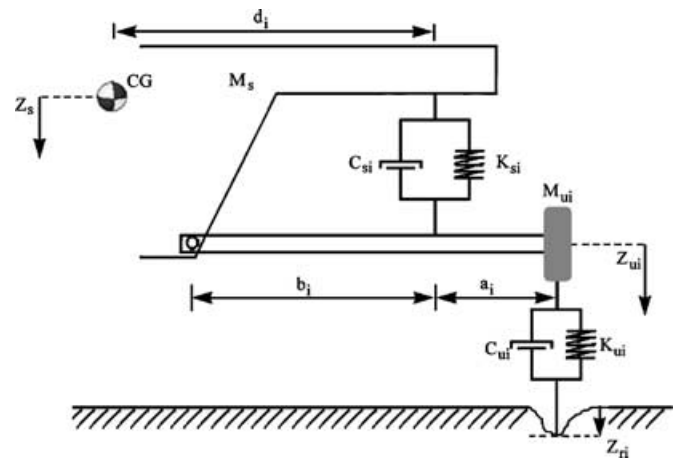

Fig. 9. The model of suspension system.

ground via the wheel virtual spring and damping (corresponding to K_{ui} and C_{ui}) and to the chassis via a spring-damping system (K_{si} and C_{si}). All four wheel-suspensions are assumed to be vertically directed. Z_s is the height of the center of gravity of the sprung mass. Z_{ui} is assigned for the height of unsprung mass and Z_{ri} is due to road roughness.

3.4. Neural Network Training

Prior to apply the yaw rate control, we should train the neural network. This goal is achieved by a simulation run. The vehicle accelerates from standstill up to a maximum speed then brakes down to standstill, while a sine-wave form driving is performed in order to excite different dynamics. Figure 10 shows the result of training process. During the training, the yaw reference generator learns to become close to the yaw rate for different vehicle speeds and steering angles.

3.5. Simulation Results

A series of computer simulations are carried out to evaluate the performance of the proposed control system. The results of simulation are explained in the following sections.

1. *Speed Estimations*: To evaluate the performance of the speed estimator, braking and acceleration on a slippery road is simulated. The vehicle is initially moving

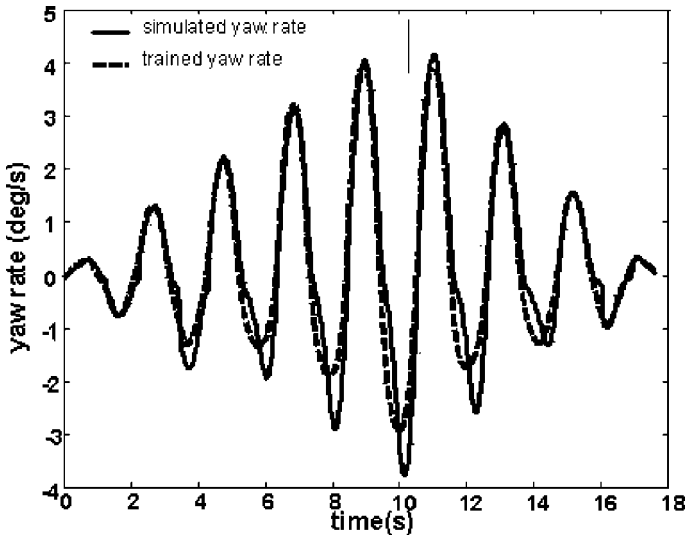

Fig. 10. Neural net training.

with a speed of 90 km/h then suddenly brakes. After 9 s the vehicle accelerates and the speed start increasing. The simulation results are shown in Figure 11. Figure 11a compares the estimated speed with the simulated true speed. In the simulation

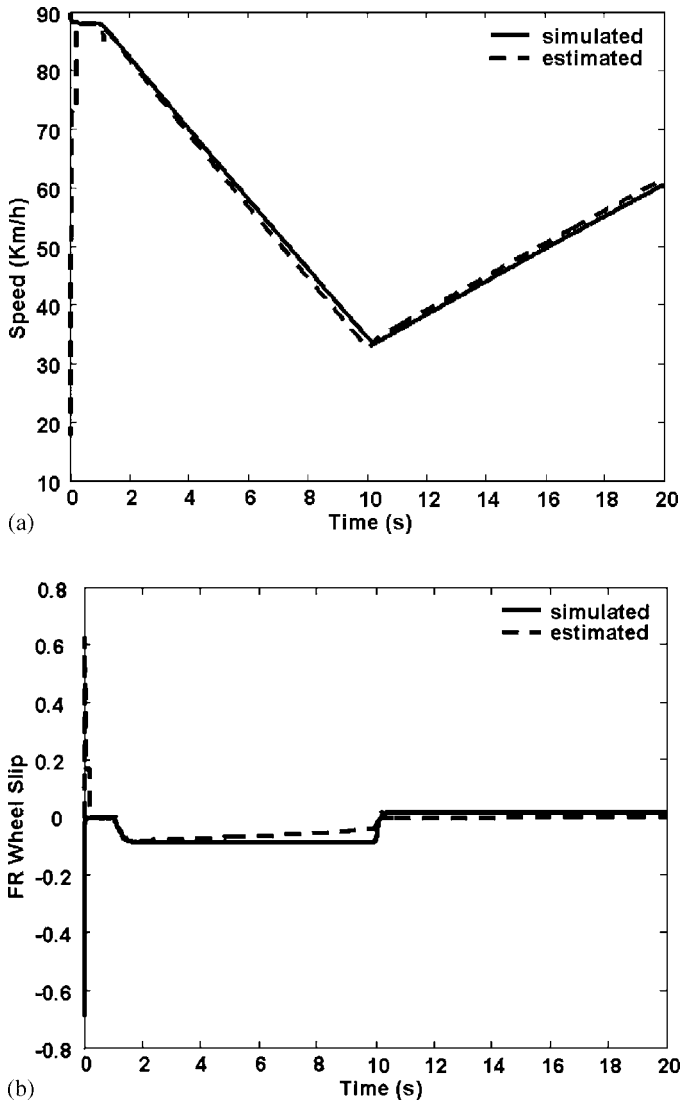

Fig. 11. Vehicle speed estimation during braking and acceleration: (a)speed, (b) FR tire slip, (c) RR tire slip.

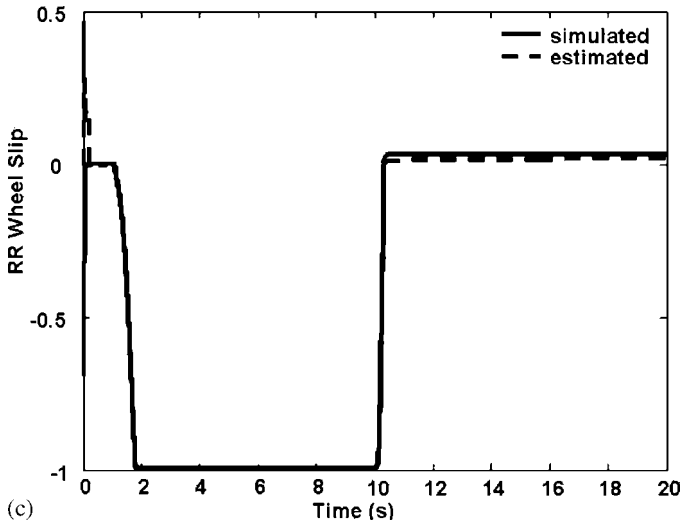

(c)

Fig. 11. (*continued*)

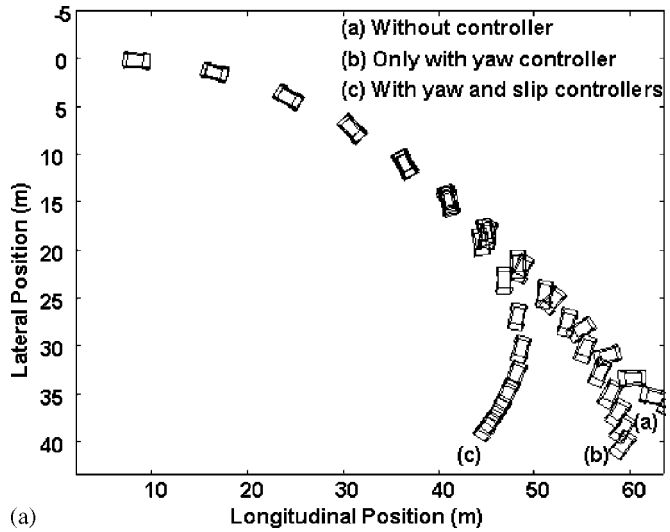

(a)

Fig. 12. Braking while turning; (a) Vehicle trajectory, (b) yaw rate, (c) side-slip angle, (d) Front-left wheel slip, (e) Front-right wheel slip.

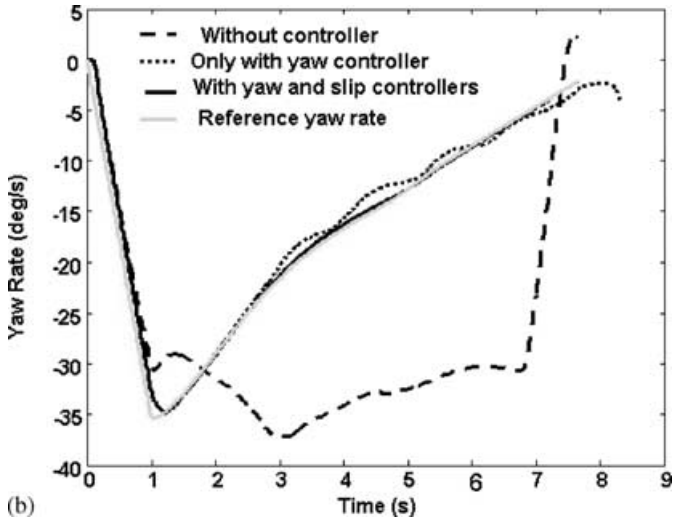

(b)

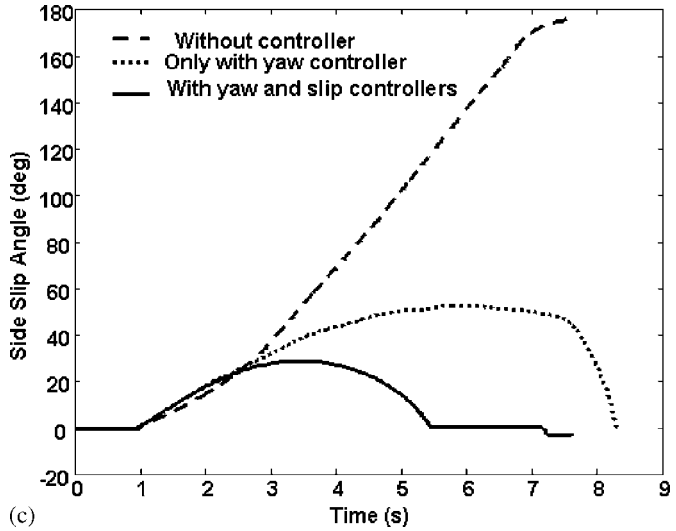

(c)

Fig. 12. (*continued*)

run the rear wheels are blocked and stop turning during the vehicle deceleration and the front wheels experience considerable slip values. Figure 11b and c show estimated slip for the front-right and the rear right wheels. The left wheels have

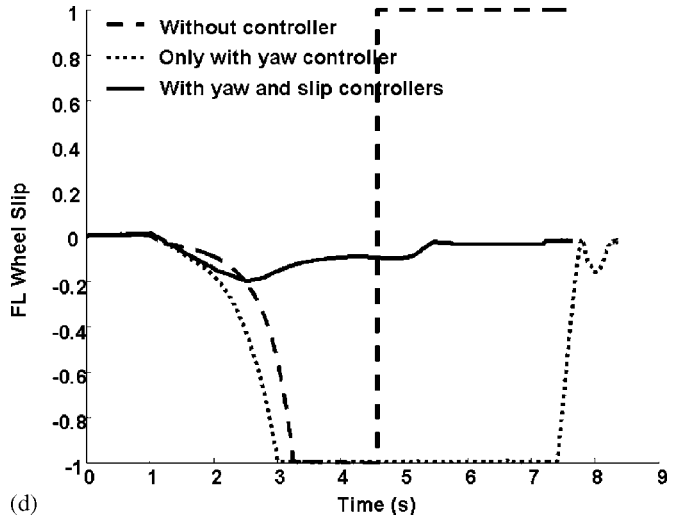

(d)

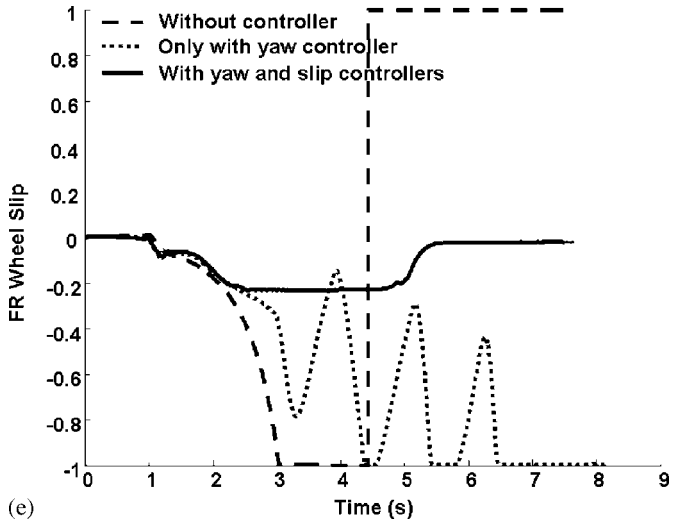

(e)

Fig. 12. (*continued*)

similar performances. Although the rear wheels blocked immediately after braking but the estimation is rather desirable.

2. *Braking While Turning*: As an example, vehicle turning while decelerating on a slippery road is examined. The vehicle initially moves with a velocity of 60 km/h.

A sudden change in steering angle amounts to a wheel turn angle of 0.1 radians. At the same time the driver induces a heavily braking to the vehicle. Figure 12 shows the simulation results. One can see in Figure 12a that the control system prevents the vehicle to spin. Without the controllers the vehicle turns around. Figure 12b compares the yaw rate with the reference value. It is clearly found that the yaw rate is nearly closed to that of desired dynamic model. Although the yaw controller itself can prevent the car from spinning but without the slip controllers the driver cannot bring the vehicle into alignment due to lack of tire lateral force. The front wheel slips are shown in Figure 12d and e. Without the slip controller, no matter whether the yaw controller is used or not, the wheels are blocked. However, with both the yaw and slip controllers, the wheel slip remain in the tire stable region, retaining steerability during turning. On the other hand, using the proposed control system, the side slip angle in the vehicle body stays definite as depicted in Figure 12c. Without the controllers the vehicle spins, hence the side slip indomitably increases.

4. CONCLUSION

A novel driver-assist stability system for all-wheel drive electric vehicles was introduced. The system adjusts the four independent electric motors to bring the vehicle into alignment with the needs of driver. The control system is based on Fuzzy logic Direct Yaw-moment Controller together with Fuzzy slip controllers for each wheel. A multi-sensor data fusion method was used in order to estimate the vehicle real speed. A sine-wave steering with varying speed was used to train the neural network, and the control system was evaluated with a braking while turning maneuver on a slippery road. The investigation with the computer simulation proved the effects of the proposed control system on improving vehicle performance under severe maneuvering conditions and preventing the vehicle from falling into a catastrophic motion. Furthermore the investigation proved the Fuzzy slip controller effectively prevents the tire skid even on icy roads.

REFERENCES

1. Yoshioka, T. et al.: Application of Sliding-mode Control to Control Vehicle Stability. In: *Proceedings of AVEC'98*, 1998.
2. Motoyama, S. et al.: Quantitive Evaluation for Yaw Control Ability. In: *Proceedings of AVEC'98*, 1998.
3. Nagai, M. et al: Integrated Control Law of Active Rear Wheel Steering and Direct Yaw Moment Control. In: *Proceedings of AVEC* 1996, pp. 451–469.
4. Shibahata, Y. et al.: The Improvement of Vehicle Maneuverability by Direct Yaw Moment Control. In: *Proceedings of AVEC'92*, 1992.

5. Matsumoto, S. et al.: Improvement of Vehicle Dynamics Through Braking Force Distribution Control. *SAE 920645*.
6. Tahami, F. et al.: Fuzzy Based Stability Enhancement System for a Four-Motor-Wheel Electric Vehicle. In: *Proceedings of the SAE Dynamics and Stability Conference*, Detroit, May 2002.
7. Tahami, F., Farhanghi, S. and Kazemi, R.: Stability Enhancement of a Two-Motor-Drive Electric Vehicle Using Fuzzy Logic [In Persian]. In: *Proceedings of the First Iranian Conference on hybrid and Electric Vehicles*, Tehran, July 2001.
8. Gillespie, T.: Fundamentals of Vehicle Dynamics. *Society of Automotive Engineers*, 1992.
9. Bakker, E., Pacejka, H.B. and Lidne, L.: A New Tire Model with an Application in Vehicle Dynamics Studies. *SAE Transactions: Journal of Passenger Cars*, 98 (1989), pp. 451–439.